FINAL VERSION SEPTEMBER 28, 2020
Preprint typeset using LaTeX style emulateapj v. 12/16/11

MONTE CARLO SIMULATIONS APPLIED TO THE PARTICLES PROPAGATING IN THE MATTER AND RELATED PROCESSES THEY UNDERGO RADIATION AND DOSIMETRY, FYS9711 PROJECT 1

MARIA MARKOVA

Final version September 28, 2020

ABSTRACT

The following project is focused on the application of the rejection technique and the inverse transform sampling for the simulation of the photon tracks in water. Two initial energies of photons are considered, 200 keV and 2 MeV. The first part of exercises includes setting of simplest code for the random number generation, further applied to the simulation of the one dimensional random walk for a particle with and without energy loss in each interaction node. the second part of the exercises is focused on the reproduction of the attenuation coefficient for 200 keV and 2 MeV photons in water, study of the probability distributions, sampling photon step lengths and photon scattering angles. All intermediate steps studies in exercises 1-8 are further applied for the simulation of the photon tracks, given the Compton interaction as the only interaction type photons undergo in water.

1. PROBLEMS COVERED BY THE EXERCISES

The following project considers a beam of photons propagating in water. The incident beam is monoenergetic and two initial photon energies are considered, 200 keV and 2 MeV. The number of electrons per volume unit in water is $n_V = 3.43 \times 10^{23} \mathrm{cm}^{-3}$. The photons are assumet to undergo the only type of interaction, the Compton scattering. This provides a simplified treatment of photons and their propagation in the matter, since the complete picture should also include the photoelectric effect and the pair production. This would allow us to study photons with lower and higher energies, for which these effects become predominant (photoeffect for lower energy photons and the pair production for higher energy photons). However, for the given energy window, the assumption of the predominant Compton scattering is fairly reasonable (see Fig.1). This part of the project is preceded by the exercises on an abstract particle in one-dimensional case undergoing random changes of direction and position, equivalent to interactions with other particles. In each interaction node, a certain amount of energy, proportional to the step length, is lost. In exercises 1-3 the position x is given in arbitrary units.

1.1. *Exercise 1: Random number generator*

It this task 1000 random numbers were sampled from two types of distributions, the uniform distribution in the left-open interval [0,1) and the Gaussian distribution, given by:

$$f(x) = \frac{1}{\sqrt{2\pi\sigma^2}} e^{-\frac{(x-x_0)^2}{2\sigma^2}}. \quad (1)$$

Here, the mean value $x_0 = 0$ and the standard deviation $\sigma^2 = 1$. This was performed by the functionalities of the *numpy* python 3 package as shown below:

maria.markova@phys.uio.no
[1] Department of Physics, University of Oslo, P.O. Box 1048 Blindern, N-0316 Oslo, Norway

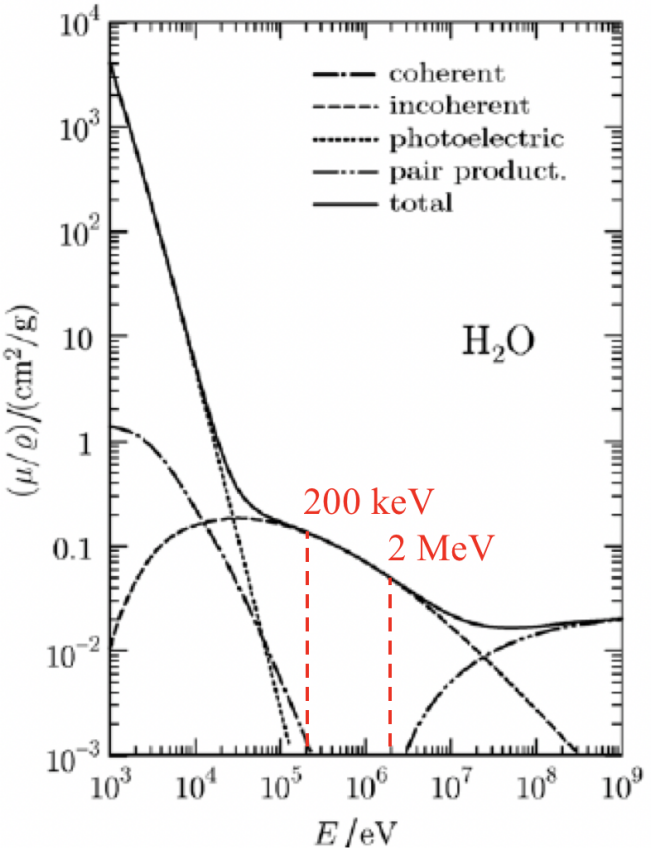

FIG. 1.— Partial and total mass attenuation coefficient of water as a function of the photon energy. Figure is taken from (1)

```
np.random.seed(2020)

uniform = np.random.uniform(0, 1, 1000)
gaussian = np.random.normal(0, 1, 1000)
```

The results of the sampling are demonstrated in the Fig.2 and Fig.3. The counts generated with the Gaus-

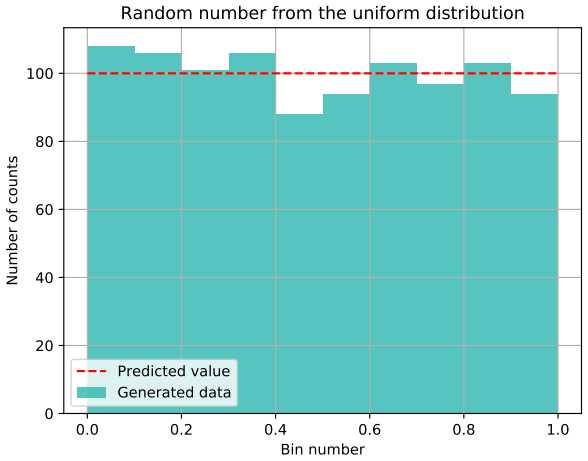

FIG. 2.— 1000 random numbers sampled from the uniform distribution, 10 bins.

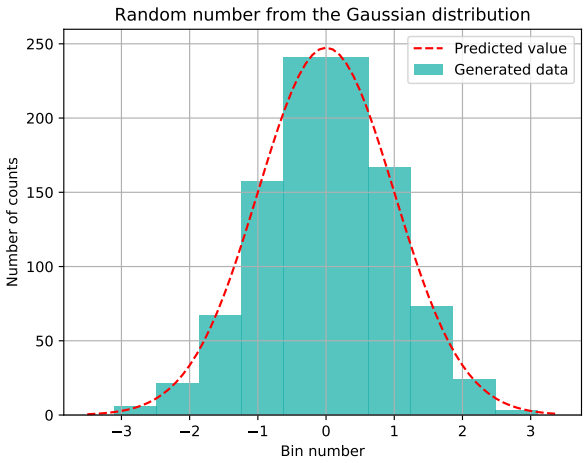

FIG. 3.— 1000 random numbers sampled from the Gaussian distribution with $\mathcal{N}(0,1)$, 10 bins.

sian distribution were additionally fitted to find the fit values of x_0 and σ. The fit results in $x_0 = 0.023(6)$ and $\sigma = 0.974(6)$ (and additional amplitude $A = 620(3)$, which correspond to the values set for the generation. The performed fit is shown in Fig.3 together with the generated data. For the counts distributed uniformly on [0,1) one can observe the fluctuation of counts in each bin around the mean value $y_{mean} = 100$, which is expected according to the stochastic nature of the generated data.

1.2. *Exercise 2: Random walk in 1 dimension*

In this exercise we consider an abstract particle able to "walk" along the x-axis with a step length distributed randomly according to the Gaussian distribution with $\mathcal{N}(0,1)$. Sampling of the step length from this distribution includes automatically a random change of direction. Due to the symmetrical distribution $\mathcal{N}(0,1)$, in 50% cases a particle continues moving forward (along x-axis), otherwise it moves in the opposite direction. The x-positions of random 10 particles out of 1000 simulated are shown in Fig.4 as functions of the collision (random change of the

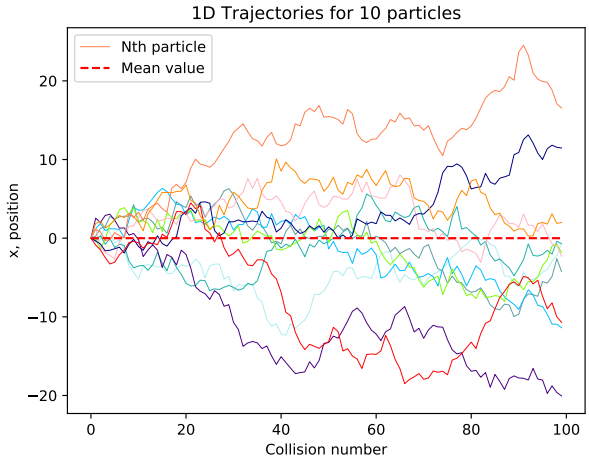

FIG. 4.— Distribution of x-positions of 10 random particles vs. collision number.

position) number. It might be inferred that the average x-position of considered particles in each collision point is close to 0. This was confirmed by plotting the final distribution of 1000 particles in form of the histogram (see Fig.5).In this case, only 100 collisions were considered, and the position distribution is plotted for the 100th collision for all simulated particles. The part of the code corresponding to this simulation is the following:

```
NumParticles = 1000
NumSteps = 100
Steps = np.arange(NumSteps)
Positions = np.zeros((NumParticles,NumSteps)
    )

for i in range(NumParticles):
        for j in range(1,NumSteps):
                step = np.random.normal(0,
                    1, 1)
                Positions[i, j]=Positions[i,
                    j-1]+step
print(len(Positions[0,:]))
```

The distribution was additionally fitted (dashed red line), providing the parameters $x_0 = 0.9(2)$ and $\sigma = 9.6(2)$, and the amplitude $A = 6807(125)$. The mean final position is indeed coincides with 0 (within the given fit error). This might be understood based of the sampling of the step length, distributed according to the Gaussian distribution with $x_0 = 0$. The distribution of the final positions follows the same Gaussian distribution with the different value of σ defined by the number of considered collisions (increasing with the increasing amount of considered steps).

1.3. *Exercise 3: Random walk in 1 dimension including energy loss*

This task is based on the simulation of a random walk for a particle performed in the previous task, but with an additional energy loss at each step included. The energy lost in each "interaction" is assumed to be proportional to the step length as $T = k\Delta s$. The initial energies of 1000 simulated particles were set to 100 a.u.. The units can be chosen to be expressed in MeV, and the proportionality coefficient k will be expressed in MeV/cm. The

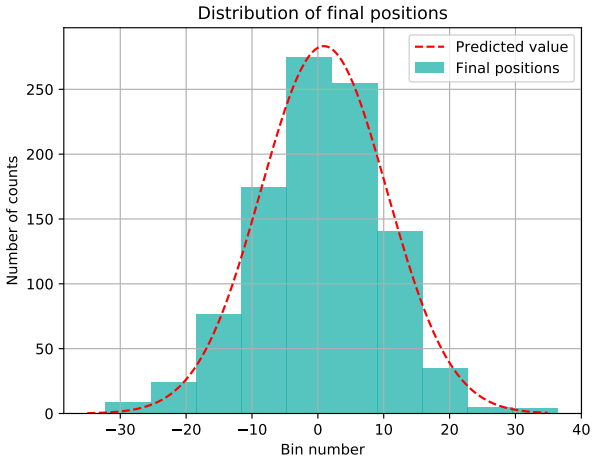

FIG. 5.— Distribution of final positions for 1000 particles, 10 bins.

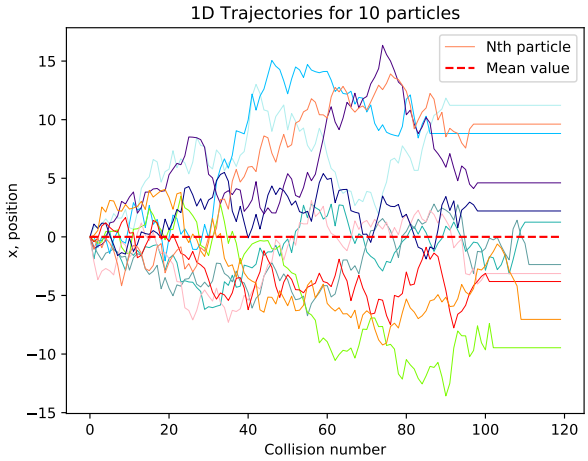

FIG. 6.— Distribution of x-positions of 10 random particles vs. collision number with energy loss.

coefficient was set so that it requires on average 100 collisions for 1000 particles to reduce the mean energy of the particle ensemble from 100 a.u. to zero. The coefficient was found to be:

$$k \approx 1.26466 \approx 1.265 \text{ MeV/cm}. \quad (2)$$

This coefficient was applied for all further calculations:

```
for i in range(NumParticles):
  for j in range(1,NumSteps):
        step = np.random.normal(0, 1, 1)
        if(Energies[i, j-1]>0):
          Positions[i, j] = Positions[i, j
              -1]+step
          Energies[i, j] = Energies[i, j-1]-
              k*abs(step)
          if(Energies[i, j]<0):
                Energies[i, j] = 0
        else:
          Positions[i, j] = Positions[i, j
              -1]
          Energies[i, j] = 0
```

Fig.6 demonstrates positions of 10 random particles plotted as functions of a collision number. The energy threshold was implemented as following: if energy of a particle after a current step becomes negative, it is set to zero and the coordinate of a particle is kept (particle has stopped).This principle is demonstrated in Fig.6, approximately half of the particles has stopped after $N < 100$ collisions, as for another half more than 100 collisions were required, keeping the average number of collisions before the full stop ≈ 100.

Figure 7 demonstrates final distribution of 1000 particles along the x-axis. This distribution follows the Gaussian distribution and was additionally fitted. The fit coefficients $x_0 = -0.2(3)$ and $\sigma = 10.1(3)$, and the amplitude $A = 6284(157)$ were used to plot the predicted value in 7. The distribution is centered at 0 by analogy with the exercise 2. Analogous position distribution in exercise 2 and 3 is expected, since the only modification in form of the added energy loss does not affect the step lengths of a particle after each collision. The only effect of the energy loss is a stop of a particle after a certain collision. As the average position of 1000 at each interaction step is expected to be 0, this should be the case for exercise 3 as well.

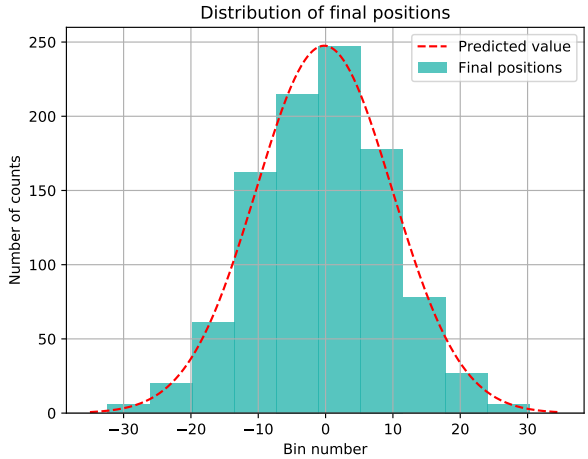

FIG. 7.— Distribution of final positions for 1000 particles, 10 bins, energy loss is included.

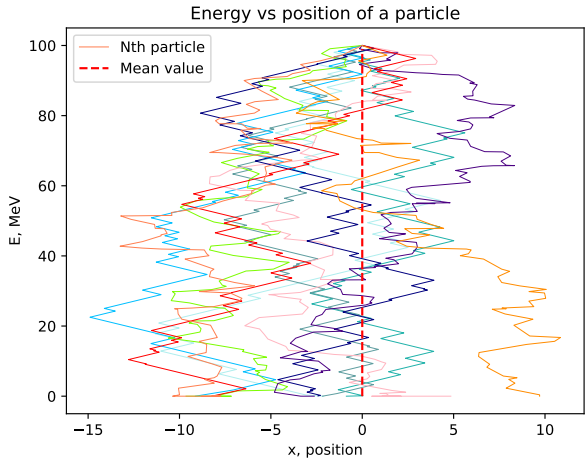

FIG. 8.— Energy loss for 10 particles vs. x-positions.

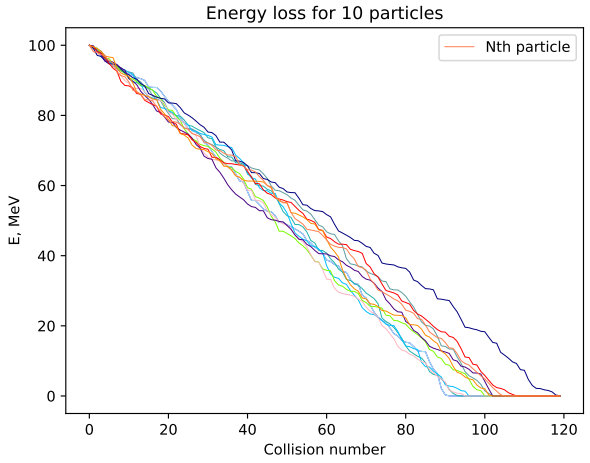

FIG. 9.— Energy loss for 10 particles vs. collision number.

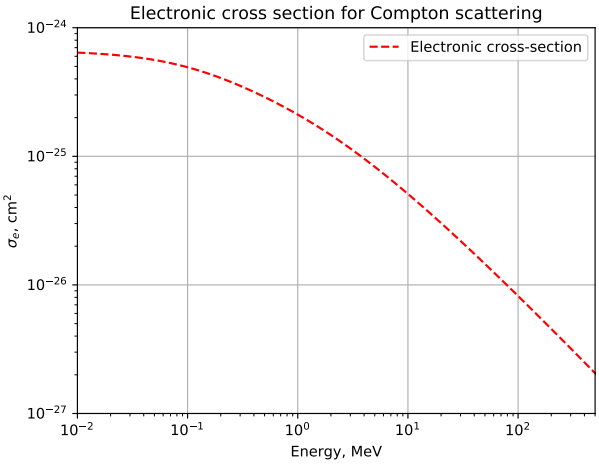

FIG. 10.— Energy dependence of the electronic cross-section for the Compton scattering for water.

Figure 8 demonstrates the gradual energy loss for 10 arbitrary particles as a function of their x positions. Upper point corresponds to the 0 position for all particles with the initial energy of 100 MeV, as the $E_{fin} = 0$ results in the same position distribution as shown in 7. Figure 9 demonstrates the gradual energy reduction for 10 particles from 100 MeV to 0 and the fact that the average number of collisions required to perform this reduction is ≈ 100 . In practice, an assumption of a constant proportionality coefficient throughout the whole process with a wide energy included is unrealistic as well as the energy-independent step length for each particle.

1.4. *Exercise 4: Attenuation coefficient function*

In the following exercise the Klein-Nishina electronic cross-section for Compton scattering was implemented as following (2):

$$\begin{aligned}\sigma_e =& 2\pi \int_{\phi=0}^{\pi} \frac{d_e\sigma}{d\Omega_\phi} \sin\phi d\phi = \\ =& \pi r_0^2 \int_0^{\pi} \left(\frac{h\nu'}{h\nu}\right)\left(\frac{h\nu'}{h\nu} + \frac{h\nu}{h\nu'} - \sin^2\phi\right)\sin\phi d\phi = \\ =& 2\pi r_0^2 \frac{1+\alpha}{\alpha^2}\left(\frac{2(1+\alpha)}{1+2\alpha} - \frac{\ln 1+2\alpha}{\alpha}\right) + \\ &+ 2\pi r_0^2 \frac{\ln 1+2\alpha}{2\alpha} - \frac{1+3\alpha}{(1+2\alpha)^2},\end{aligned} \tag{3}$$

where $r_0 = 2.818 \times 10^{-13}$ cm is the classical electron radius, $\alpha = \frac{h\nu}{m_e c^2} = \frac{h\nu}{0.511\ \text{MeV}}$, $h\nu$ is the current photon energy. The electron cross-section is shown in Fig.10. The cross-section is in a complete agreement with the Fig.7.6 from (2). Further, the Compton mass attenuation coefficient was obtained as (2):

$$\frac{\sigma}{\rho} = \frac{N_A Z}{A}\sigma_e, \tag{4}$$

where $N_A = 6.02 \times 1023\ \text{mol}^{-1}$. The mass attenuation coefficients were calculated as a function of photon energy for both oxygen and hydrogen atoms. Based on the assumption of the predominant Compton interaction,

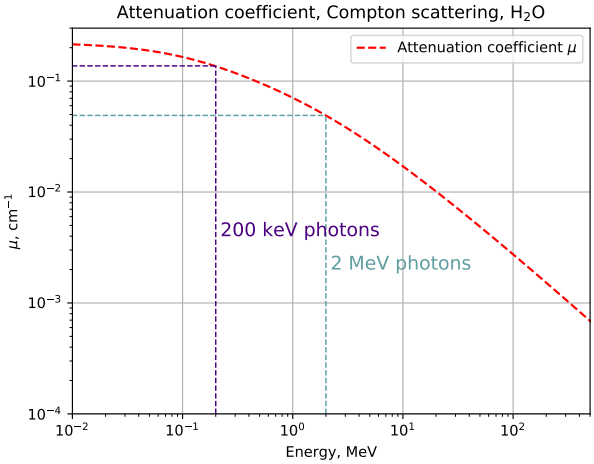

FIG. 11.— Energy loss for 10 particles vs. collision number.

one can write the total mass attenuation coefficient:

$$\frac{\mu}{\rho} = \frac{\sigma}{\rho}. \tag{5}$$

For the mixture of atoms the total mass attenuation coefficient might be written as:

$$\frac{\mu}{\rho}_{H_2O} = f_O \frac{\mu}{\rho}_O + f_H \frac{\mu}{\rho}_H \approx \frac{16}{18}\frac{\mu}{\rho}_O + \frac{2}{18}\frac{\mu}{\rho}_H, \tag{6}$$

where f_O and f_H are the weight coefficients. Finally, the linear attenuation coefficient (cm^{-1}) for water was obtained by multiplying the obtained total mass attenuation coefficient (cm^2/g) by the density of water, $\rho_{H_2O} = 1\ \text{g/cm}^3$. Figure 11 displays the energy dependence of the linear attenuation coefficient μ for water. For two reference energies, 200 keV and 2 MeV, the coefficients are $\mu = 0.1359 \approx 0.136\text{cm}^{-1}$ and $\mu = 0.0489 \approx 0.049\text{cm}^{-1}$ correspondingly. Both numbers are in a good agreement with the reported values (3).

1.5. *Exercise 5: Probability distributions*

The linear attenuation coefficients obtained in the previous task were used to compute the probability distribu-

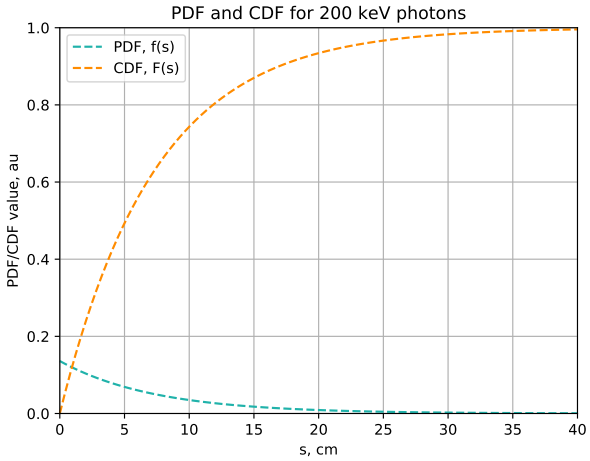

FIG. 12.— Probability distribution function and cumulative distribution function for 200 keV photons.

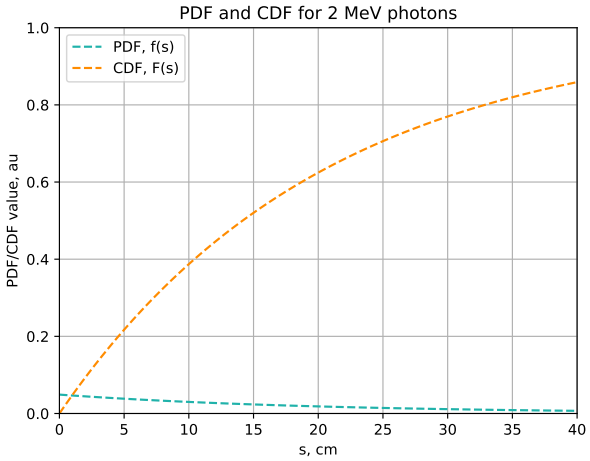

FIG. 13.— Probability distribution function and cumulative distribution function for 2 MeV photons.

tion function for 200 keV and 2 MeV photons. Since the probability density function for finding a certain number of photons at a given depth might be represented as:

$$f(x) \sim e^{-\mu x}, \tag{7}$$

normalization of this function results in:

$$1 = C \int_0^\infty e^{-\mu x} dx \Rightarrow C = \mu. \tag{8}$$

The complete form of the probability distribution function (PDF) is:

$$f(x) = \mu e^{-\mu x}. \tag{9}$$

The probability distribution function for both 200 keV and 2 MeV photons is shown in Fig.12 and Fig.13. The cumulative distribution function (CPD) can thus be defined as:

$$F(s) = \int_0^s \mu e^{-\mu x} dx = 1 - e^{-\mu s}. \tag{10}$$

The cumulative probability distribution for 200 keV and 2 MeV photons are shown together with the corresponding PDFs in Fig.12 and Fig.13.

1.6. *Exercise 6: Sampling photon step lengths using the inverse transform*

Both the PDF and the CPD functions obtained in the previous task could be used for sampling the path lengths for 200 keV and 2 MeV photons using the inverse transform technique. The CPD is a monotonously increasing function of s, increasing from 0 value at $s = 0$ to 1 at $s \leftarrow \infty$. Sampling a ramdom number ξ from the uniform distribution on [0,1) interval provides us with randomly sampled values of the CDF. Unisng the inverse transformation from $F(s)$ to s one gets:

$$s(\xi) = -\frac{\ln 1 - \xi}{\mu}, \tag{11}$$

where s is equivalent to the step length. 1000 photons with initial energies of 200 keV and 2 MeV were used for the above described sampling of the path lengths. The part of the code performing the samplibg is the following:

```
NumSim = 1000
Pathlengths = np.zeros(NumSim)

for i in range(NumSim):
        ksi = np.random.uniform(0,1,1)
        Pathlengths[i] = - np.log(1-ksi)/
            mu_tot
```

The results of the sampling are shown in Fig.14 and Fig.15 together with the exponential fit. The expected value of the mean free path is given by:

$$l_{MFP} = \frac{1}{\mu}, \tag{12}$$

corresponding to 7.002 cm and 20.857 cm for 200 keV and 2 MeV photons respectively. The mean value obtained with the sampling procedure are $l_{MFP}(200\text{ keV}) = 7.353$ cm and $l_{MFP}(2\text{ MeV}) = 20.422$ cm. These values are essentially close to those obtained by the inversion of the calculated linear attenuation coefficients. The mean values can be improved significantly with the increasing number of sampled photons (e.g. 100000 or 1000000). In overall, the sampled path lengths follow the predicted analytical form of the PDF $f(x) \sim e^{-\mu x}$.

1.7. *Exercise 7: Normalized differential scattering cross section*

In this exercise the differential Compton scattering cross-section is modelled. Differential Compton cross-section (with respect to the solid angle $d\Omega$) is given by (2):

$$\left(\frac{d\sigma}{d\Omega}\right) = \frac{r_0^2}{2}\left(\frac{h\nu}{h\nu'} + \frac{h\nu'}{h\nu} - \sin^2\theta\right), \tag{13}$$

where the energy of a scattered photon is given by:

$$h\nu' = \frac{h\nu}{1 + \frac{h\nu}{mc^2}(1 - \cos(\theta)}. \tag{14}$$

Given the differential solid angle $d\Omega = 2\pi \sin\theta d\theta$ (uniform distribution over azimuthal angles is assumed), the cross-section can be modified into the differential cross-

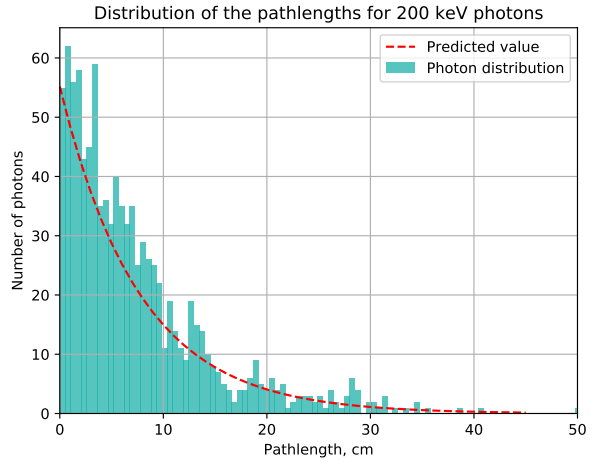

FIG. 14.— Distribution of the path lengths for 200 keV photons sampled with the inverse transform technique.

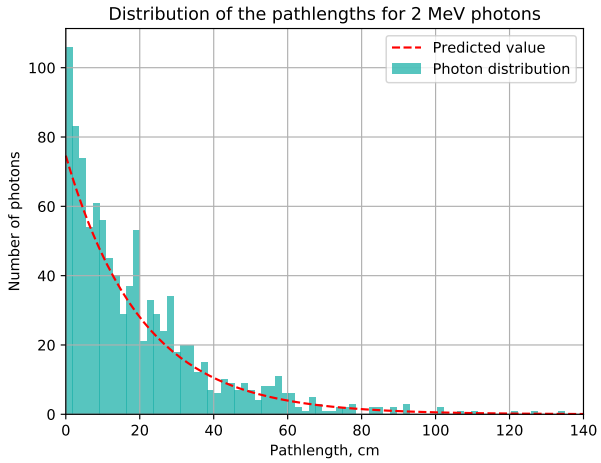

FIG. 15.— Distribution of the path lengths for 2 MeV photons sampled with the inverse transform technique.

section with respect to the polar angle θ:

$$\left(\frac{d\sigma}{d\Omega}\right) = \pi r_0^2 \left(\frac{h\nu}{h\nu'} + \frac{h\nu'}{h\nu} - \sin^2\theta\right) \sin\theta. \qquad (15)$$

This form of the differential cross-section was computed for 200 keV photons and 2 MeV photons and normalized by the maximum value of each cross-section. Cross-sections are presented in Fig.16 and Fig.17.

The normalised differential cross-sections reflect the relative probability of a photon to be scattered in a certain angle. It can be seen from Fig.17 that the forward direction becomes preferable as the energy of a photon increases.

1.8. *Exercise 8: Sampling Compton scattering angles using the rejection technique*

In the following task the normalized differential Compton cross-sections were used for sampling the scattering angles of photons. Since the cross-section is a finite function on the interval $\theta \in [0,180°]$ and can be easily normalized to 1 for both axes, it is convenient to apply the rejection technique. The first step implies generation of two uniformly distributed numbers ξ and χ corresponding to normalized x and y coordinates. Secondly, the check is carried out: if the corresponding ordinate χ lies within the area confined by the normalized cross-section, the abscissa ξ is kept and further converted into a sampled angle $\theta = 180\xi$. Otherwise the sampled pair of numbers is rejected. In order to gain sufficient statistics (rejection is included), the amoutnt of sampled photons is increased by 2 (the cross-section divides the 1×1 square by roughly equal parts). The part of the code performing the sampling is the following:

```
for i in range(NumPhot):
        x_tr = np.random.uniform(0,1,1)
        y_tr = np.random.uniform(0,1,1)
        theta_tr = x_tr*180
        Escat = Einit/(1+Einit/0.511*(1-np.
            cos(theta_tr*math.pi/180)))
        xs_tr = math.pi*(2.818e-13)**2*(
            Escat/Einit)**2*(Einit/Escat+
            Escat/Einit-np.sin(theta_tr*math
            .pi/180)**2)*np.sin(theta_tr*
            math.pi/180)/np.max(
            d_sigma_d_theta)
        if(y_tr<=xs_tr):
                n=n+1
                thetas.append(180*x_tr)
```

The resulting sampled angles are saved and presented in the form of the histogram in Fig.18 and Fig.19 for 200 keV and 2 MeV photons. The sampled angles follow the predicted differential cross-section and reflect the same principle of dominating forward angles for a higher photon energy.

1.9. *Exercise 9: Photon trajectory simulation*

Final task aims at combining all studied techniques (rejection and inverse transform techniques) in order to reproduce realistic paths of 200 keV and 2 MeV photons in water. In both cases 1000 photons are considered. For each particle an initial energy is attributed and all calculations are performed in the while loop stopping the calculations when the current energy for a given particle is below a 50 keV threshold. First of all, the linear attenuation coefficient is modelled for a current particle

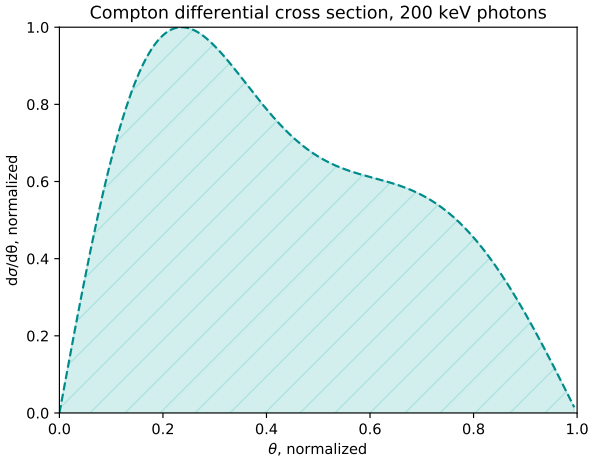

FIG. 16.— Normalized differential Compton cross-section for 200 keV photons.

energy and used for the inverse transform sampling of

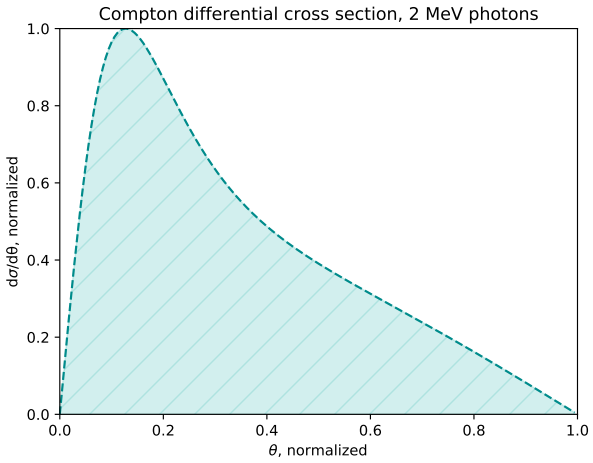

FIG. 17.— Normalized differential Compton cross-section for 2 MeV photons.

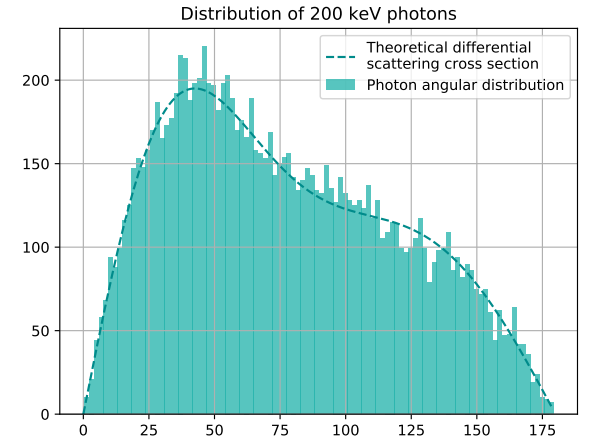

FIG. 18.— Angles for 200 keV photons sampled with the rejection technique.

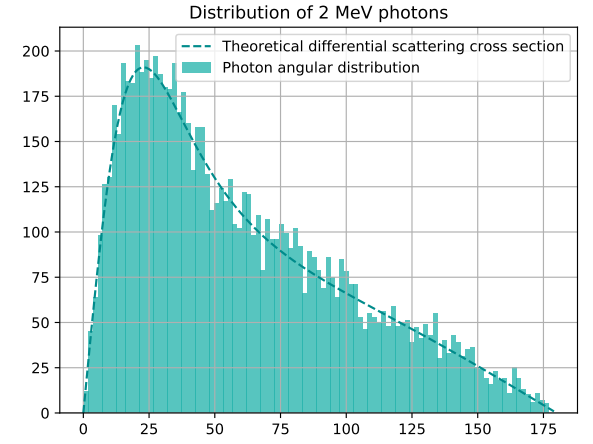

FIG. 19.— Angles for 2 MeV photons sampled with the rejection technique.

the path length by analogy with the exercise 6. Further, the normalized differential Compton cross-section is modelled and used for the application of the rejection technique for sampling of the polar angles θ for each particle. However, the polar angles are provided for a reference frame related to a given photon. An additional transformation to the laboratory frame of reference is required and was performed as:

$$\cos\theta_{n+1} = \sin\theta_s \cos\phi_s \sin\theta_n + \cos\theta_s \cos\theta_n, \qquad (16)$$

where θ_s is the scattering angle found with the sampling, θ_n and ϕ_n are polar and azimuthal angles for a given photon in the laboratory frame. As the new scattering angle in the laboratory frame is found, the current positions of the particles are updated as:

$$\begin{aligned} x_{n+1} &= x_n + \delta s \sin\theta_{n+1} \cos\phi_{n+1}, \\ y_{n+1} &= y_n + \delta s \sin\theta_{n+1} \sin\phi_{n+1}, \\ z_{n+1} &= z_n + \delta s \cos\theta_{n+1}, \end{aligned} \qquad (17)$$

where δs is the sampled step length. Azimuthal symmetry is taken into account and the new angle ϕ_{n+1} is sampled from the normal distribution [0,2π]. The photons are generated randomly on the 10cm $\times$ 10 cm surface in the x-y plane.

The x-z projections of the trajectories are shown in Fig.20 and Fig.21. It can be seen that the higher energy photons are able to propagate further in water as compared to 200 keV photons. In addition, dominating forward direction of 2 MeV photons is clearly seen in Fig.21.In overall, the first step made by initial 2 MeV or 200 keV photons is significantly larger than all following steps, as it should be expected from photons, gradually loosing energy in water as they propagate further. This is also clearly demonstrated by both figures.

In addition, the x-y projections of the trajectories for 100 particles are presented in Fig.22 and Fig.23. In both cases, no predominant direction can be distinguished. Indeed, the azimuthal symmetry implemented in the code via normally distributed azimuthal angles is clearly seen. The only predominant direction (along the z axis) is aligned with the initial radius vectors of photons. This direction could have been even more distinct in the figure if more particles (e.g. 1000000) were considered. The same applies to the uniform distribution in the x-y plane.

Finally, the mean energy of all generated photons is plotted as a function of the distance ($r = \sqrt{x^2 + y^2 + z^2}$ from the generation area (see Fig.24 and Fig.25). It can be seen that at the generation surface all particles have the same energy, 200 keV or 2 MeV, and it decreases gradually as photons propagate further in the matter. As we reach the distance of $\approx$ 30 cm and 50 cm no photons with energy above the threshold can be found.

2. APPENDIX: LINK TO ALL PROGRAMS

Link to the project in Github

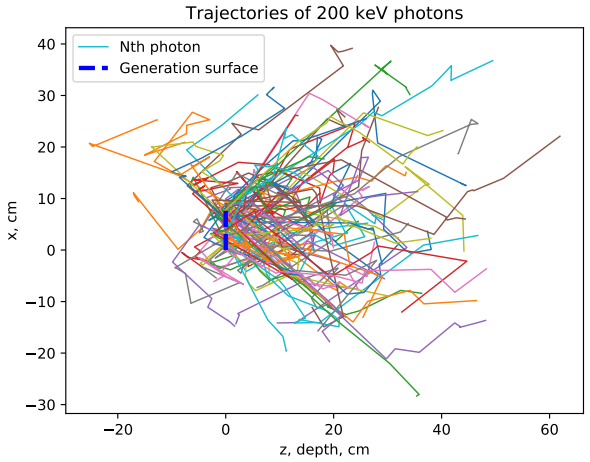

FIG. 20.— x-z projection of the trajectories for 1000 200 keV photons.

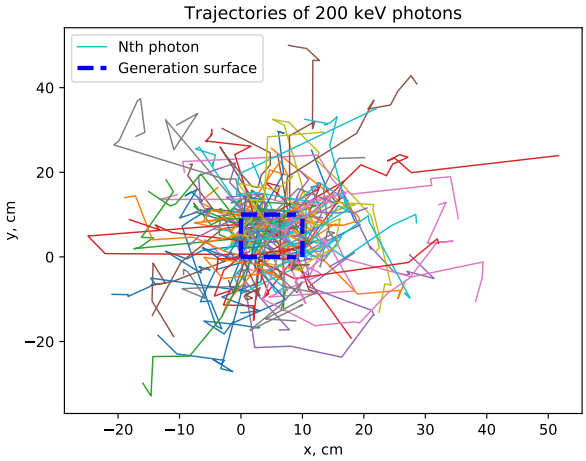

FIG. 22.— x-y projection of the trajectories for 1000 200 keV photons.

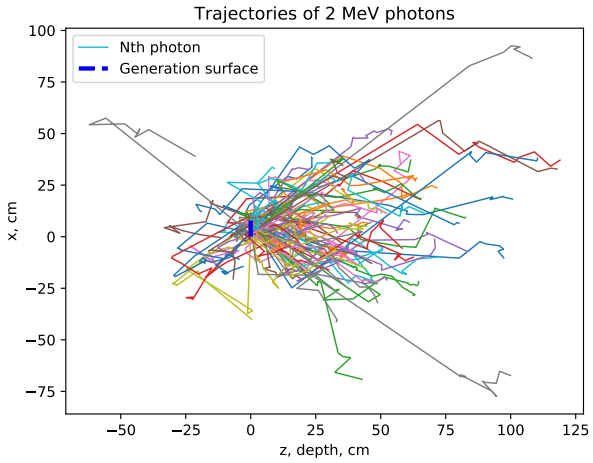

FIG. 21.— x-z projection of the trajectories for 1000 2 MeV photons.

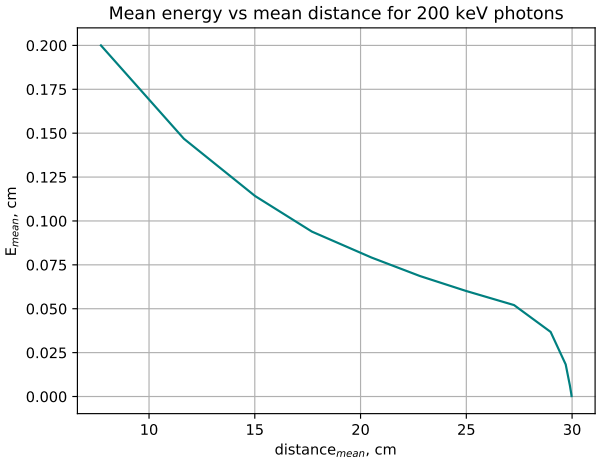

FIG. 24.— Mean energy of 200 keV photons as a function of the distance from the generation area.

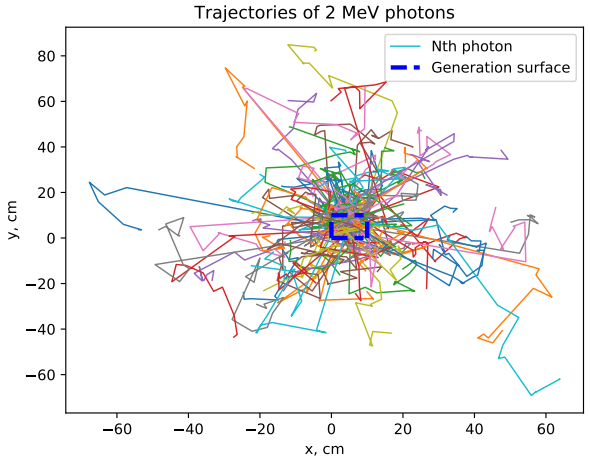

FIG. 23.— x-y projection of the trajectories for 1000 2 MeV photons.

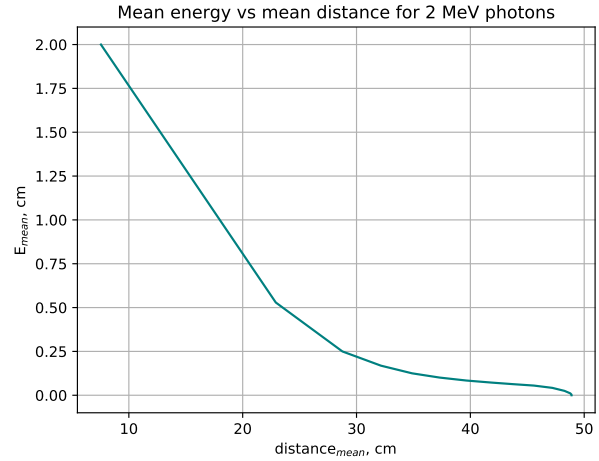

FIG. 25.— Mean energy of 2 MeV photons as a function of the distance from the generation area.

REFERENCES

[1]F. Salvat, J. M. Fernandez-Varea //Overview of physical interaction models for photon and electron transport used in Monte Carlo codes, Metrologia, V. 46, N.2, 2009.

[2]F. H. Attix// Introduction to Radiological Physics and Radiation Dosimetry, WILEY-VCH Verlag GmbH Co. KGaA, Weinheim, 2004.

[3]NIST, X-Ray Mass Attenuation Coefficients: Link to the NIST page.